Binding of Vinblastine to Phosphocellulose-Purified and αβ-Class III Tubulin: The Role of Nucleotides and β-Tubulin Isotypes†

Sharon Lobert,*,‡ Anthony Frankfurter,§ and John J. Correia||

School of Nursing and Department of Biochemistry, University of Mississippi Medical Center, Jackson, Mississippi 39216, and Department of Biology, University of Virginia, Charlottesville, Virginia 22901

Received February 7, 1995; Revised Manuscript Received April 10, 1995⊗

ABSTRACT: Vinblastine is an antimitotic drug that inhibits microtubule assembly and induces the self-association of tubulin into coiled spiral aggregates. Previous quantitative binding and sedimentation velocity results have been interpreted by a mechanism involving isodesmic ligand-mediated plus ligand-facilitated self-association [Na, G., & Timasheff, S. N. (1986) *Biochemistry 25*, 6214−6222, 6222−6228]. In this study, the vinblastine-induced self-association of porcine brain tubulin has been compared in the presence of 50 μM GDP or 50 μM GTP to investigate the role of nucleotides. Experiments at 1−4 μM tubulin in 10 mM Pipes, 1 mM $MgSO_4$, 2 mM EGTA (pH 6.9), and varying concentrations of vinblastine (0.05−70 μM) demonstrate that GDP enhances self-association by 2−4-fold over GTP. In the presence of GDP or GTP, sedimentation velocity data can be best fit by either an indefinite ligand-mediated model or an indefinite ligand-mediated plus ligand-facilitated model. The association constant, K_2, for the vinblastine−tubulin complex binding to a polymer is larger when GDP is present, while the association constant, K_1, for the binding of vinblastine to tubulin heterodimers is identical in the presence of either nucleotide. The enhancement of K_2 by GDP is confirmed by micropartition binding experiments with [^{3}H]vinblastine. The fitting of sedimentation velocity and binding studies gives parameters for the interaction of vinblastine with GTP-tubulin that are identical, within error, to the previous results of Na and Timasheff. van't Hoff analysis of multiple temperature data reveals that this enhancement in the presence of GDP is due to a change in the enthalpy of self-association. Additional results suggest that the interaction of vinblastine with tubulin is identical for all β-isotypes. Sedimentation velocity experiments in the presence of GDP or GTP show that the vinblastine-induced association of affinity-purified αβ-class III tubulin is identical to that of unfractionated tubulin, although there is a difference in the abilities of unfractionated tubulin and αβIII-tubulin to associate into taxol-stabilized microtubules.

The antimitotic and antitumor activity of vinblastine originates through its inhibition of microtubule dynamics and assembly. Vinblastine, at substoichiometric levels *in vitro*, stabilizes microtubules, possibly by binding to microtubule ends and inhibiting hydrolysis of GTP (Toso et al., 1993; Jordan et al., 1991; Jordan & Wilson, 1990). It is hypothesized that this effect on the dynamics of mitotic spindles results in the observed arrest of cell division at metaphase. Stoichiometric drug concentrations cause microtubules to depolymerize. The binding of vinblastine to tubulin heterodimers and microtubules has been investigated extensively. There is one high-affinity vinblastine binding site and two or more weak nonspecific binding sites (Na & Timasheff, 1986a,b). Binding to the high-affinity site induces indefinite isodesmic self-association of tubulin (Na & Timasheff, 1980a,b, 1986a). Na and Timasheff (1986a) demonstrated, through application of Wyman linkage theory, that a combined ligand-mediated plus ligand-facilitated model best fit the vinblastine binding data. Quantitative fitting and simulation revealed that the affinity, K_1, of vinblastine for the tubulin heterodimers is 3.8×10^5 M^{-1}, whereas the self-association of the vinblastine−tubulin complex occurs with an affinity, K_2 of 5.2×10^5 M^{-1}. In addition, there are two weak binding sites, K_0 of affinity 5×10^3 M^{-1}.

Magnesium, which induces tubulin aggregation (Frigon & Timasheff, 1975a,b), also enhances vinblastine-induced tubulin self-association (Na & Timasheff, 1986b). In fact, drug-induced association is acutely sensitive to solution conditions, including the type of buffer and the ionic strength (Na & Timasheff, 1986b; Singer et al., 1988). A review of reported binding constants demonstrated that all were determined in the presence of GTP with or without magnesium, in Mes, Pipes, or sodium phosphate buffers at 10−100 mM concentration and between pH 6.5 and 7.0 (Himes, 1991). However, it is well-known that GTP enhances microtubule formation while GDP does not. Furthermore, Howard and Timasheff (1986) demonstrated that GTP− and GDP−tubulin differ in their ability to associate into rings. GDP−tubulin is more ring-prone and thus more likely to form single- or two-layered rings at low ionic strength (10 mM sodium phosphate, pH 7.0). Similar to vinblastine-induced tubulin self-association, GDP−tubulin ring formation is enhanced by high magnesium concentrations (Howard & Timasheff, 1986). Thus, nucleotides may be important effectors of vinblastine−tubulin interaction.

† This work supported by NIH Grants NR00056 (S.L.), NS21142 (A.F.), GM41117 (J.J.C.), and BIR9216150 (J.J.C.).

* Author to whom correspondence should be addressed: School of Nursing, University of Mississippi Medical Center, 2500 N. State St., Jackson, MS 39216; telephone 601-984-6217.

‡ School of Nursing, University of Mississippi Medical Center.

§ University of Virginia.

|| Department of Biochemistry, University of Mississippi Medical Center.

⊗ Abstract published in *Advance ACS Abstracts,* June 1, 1995.

0006-2960/95/0434-8050$09.00/0

We present here a comparison of vinblastine binding to phosphocellulose-purified tubulin in the presence of GDP or GTP. At various drug concentrations, we carried out sedimentation velocity experiments and micropartition experiments with [^{3}H]vinblastine. We obtained comparable fits of sedimentation data with either the ligand-mediated or the ligand-mediated plus ligand-facilitated model for self-association. We found that GDP enhances drug-induced association through an effect primarily on K_2, the constant for self-association of vinblastine−tubulin complexes. These results were confirmed by micropartition experiments with [^{3}H]vinblastine. In addition, we explored whether the isotype composition of the subunit pool had any effect on the interaction of vinblastine with tubulin by purifying a single β-tubulin isotype, βIII. We separated βIII-tubulin with associated α-tubulin subunits from the tubulin subunit pool by a novel immunoaffinity chromatography procedure and studied vinblastine-induced self-association of the purified material in the presence of GDP or GTP. Although electron microscopy experiments suggest a magnesium dependence for taxol polymerization of αβIII heterodimers that is not present in unfractionated tubulin, we found no difference in vinblastine-induced association with either nucleotide when αβIII was compared to unfractionated tubulin. GDP enhanced vinblastine-induced association of αβIII-tubulin in a manner similar to unfractionated tubulin.

MATERIALS AND METHODS

Reagents. Deionized (Nanopure) water was used in all experiments. $MgSO_4$, EGTA,[1] GDP (type I), GTP (type II-S) glutaraldehyde, L-histidine, L-glutamate, Nonidet, and Pipes were all purchased from Sigma Chemical Company. Tris, 2-mercaptoethanol, and polyacrylamide were from Fisher Biotech. SDS (95%) was purchased from Mallinckrodt. Ampholines were purchased from Pharmacia LKB Biotechnology, Inc., and urea (ultrapure) was from Research Organics. Sephadex G-50 was from Pharmacia. The polyvinyl formal solution in ethylene dioxide and the uranyl acetate for electron microscopic experiments were from Polysciences, Inc. BCIP, NBT, and goat anti-mouse alkaline phosphatase-conjugated antibodies were from Bio-Rad. Nonradioactive vinblastine sulfate was purchased from Sigma, and [^{3}H]vinblastine sulfate (93.6% radiopurity, 11.2 Ci/mmol) was from Amersham.

Peptides. The 14-amino acid peptide identical to the carboxy terminus of βIII-tubulin (YEDDDEESEAQGPK, >95%) was synthesized by Chiron Mimotopes Peptide Systems. This peptide was used for elution of the βIII-isotype from the immunoaffinity column. The anti-βIII monoclonal antibody, TUJ1, recognizes at least four amino acids of this peptide (Lee et al., 1990). The peptide unique to the β-class II isotype CEEEEGEDEA, was >95% pure, and the sequence was verified by mass spectroscopy (data not shown). This peptide was used in preparing the monoclonal antibody, 7B9, that uniquely reacts with class II β-tubulin, as verified by competitive ELISAs with peptides for all classes of β-tubulin.

Tubulin Purification. MAP-free pig brain tubulin was obtained by two cycles of warm−cold polymerization−depolymerization followed by phosphocellulose chromatography to separate tubulin from MAPs (Williams & Lee, 1982; Correia et al., 1987). Protein concentrations were determined spectrophotometrically (Detrich & Williams, 1978) (ϵ_{278} = 1.2 L/g·cm) or by the method of Bradford (1976) calibrated with tubulin.

Purification of αβIII-Tubulin. Immunoaffinity columns were prepared by using the βIII-tubulin monoclonal antibody TUJ1 (Lee et al., 1990) coupled to protein A−agarose (Affinica Antibody Orientation Kit from Schleicher and Schuell). Unfractionated tubulin (10−15 mg) was loaded onto a 2−3 mL column at 4 °C and left for 30 min. The void volume was collected and the column was washed with 250 mM NaCl (100 mM Pipes (pH 6.9), 2 mM EGTA, 1 mM $MgSO_4$, and 0.1 mM GTP) followed by 500 mM NaCl in the same buffer. The column was mixed with 6 mM βIII peptide (final concentration 2 mM peptide) and slowly rocked at 4 °C for 2 h. The αβ-class III isotype was then eluted with 100 mM Pipes (pH 6.9), 2 mM EGTA, 1 mM $MgSO_4$, and 0.1 mM GTP. The void fractions containing the isotype were immediately equilibrated into appropriate buffers using Sephadex G-50 spun columns. This method permitted the recovery of 60−70% of the bound class III β-tubulin. Elution with a smaller peptide, seven amino acids (SEAQPK), was also tried; however, only 20% recovery of the isotype was obtained with 2 mM final peptide concentration.

Isoelectric Focusing and Western Blotting. For analysis of the void and bound fractions from immunoaffinity columns, we used SDS−PAGE followed by Western blotting to PVDF (Towbin, 1979). We have previously described our method for isoelectric focusing in vertical slab gels and subsequent wet electrotransfer to PVDF filters (Lobert & Correia, 1994).

[^{3}H]Vinblastine Binding. Ultrafiltration (Amicon Micropartition System, MPS-1) was used for binding experiments with unfractionated tubulin (2 μM) and [^{3}H]vinblastine (Sophianopoulos et al., 1978). Tubulin samples (1 mL) in 10 mM Pipes (pH 6.9), 2 mM EGTA, 1 mM $MgSO_4$, and 0.1 mM GDP or GTP with [^{3}H]vinblastine (0.05−50 μM) were prepared and left on ice for 1 h. Vinblastine concentrations were determined spectrophotometrically, ϵ_{320} = 4642 M^{-1} cm^{-1} (Lee et al., 1975). A volume of 200 μL of the sample was left on ice, and 800 μL was loaded into an Amicon filtration tube and spun at 2000 rpm for 5 min at 4 °C in a Beckman Type 20 rotor. About 200 μL spun through the filter, and from this amount 50 μL aliquots were pipeted in duplicate into 10 mL of Scintiverse (Fisher Biotech) for scintillation counting to obtain the free drug concentration. From the 200 μL sample that was not spun, 50 μL aliquots in duplicate were used for scintillation counting to determine the total drug (bound plus free).

Sedimentation Velocity Experiments. Sedimentation studies were done in a Beckman Optima XLA analytical ultracentrifuge equipped with absorbance optics and an An60 Ti rotor. Self-association of unfractionated and purified αβ-class III tubulin in the presence of vinblastine and GDP or GTP was studied by sedimentation velocity. The concentration of unfractionated tubulin was 1, 2, or 4 μM and the concentration of αβIII-tubulin was 1 μM. αβIII-Tubulin was used immediately after elution from the immunoaffinity column. For GDP experiments, tubulin samples were

[1] Abbreviations: BCIP, 5-bromo-4-chloro-3-indolyl phosphate; EGTA, [ethylenebis(oxyethylenenitrilo)]tetraacetic acid; MAP, microtubule-associated protein; NBT, nitroblue tetrazolium; PAGE, polyacrylamide gel electrophoresis; PC-tubulin, phosphocellulose-purified tubulin; Pipes, piperazine-*N*,*N*′-bis(2-ethanesulfonic acid); PVDF, poly(vinylidene difluoride); SDS, sodium dodecyl sulfate.

equilibrated (using spun Sephadex G50 columns) first into 10 mM Pipes (pH 6.9) and 2 mM EGTA to remove bound exchangeable site GTP (Correia et al., 1987) and then into 10 mM Pipes (pH 6.9), 2 mM EGTA, 1 mM $MgSO_4$, 50 μM GDP, and vinblastine concentrations ranging from 0.05 to 70 μM. The free drug concentration was obtained from the known drug concentration in the equilibration buffer. After equilibration, the protein was brought to the desired final concentration by dilution with the equilibration buffer. In these experiments the vinblastine concentration was generally in excess over tubulin, and thus this procedure, unlike the procedure of Na and Timasheff (1986a), was found to not significantly change the concentration of free vinblastine. For GTP experiments, tubulin samples were equilibrated first into 10 mM Pipes (pH 6.9), 2 mM EGTA, and 1 mM $MgSO_4$ and then into 10 mM Pipes (pH 6.9), 2 mM EGTA, 1 mM $MgSO_4$, 50 μM GTP, and the same vinblastine concentrations as used for the GDP experiments. Samples were spun in a Beckman XLA analytical ultracentrifuge at 5, 24.6, of 35.5 °C and 30 000 or 42 000 rpm. Temperature was calibrated by the method of Liu and Stafford (1995).

Velocity data were collected at an appropriate wavelength (230−280 nm), depending upon the initial concentration of the protein, and at a spacing of 0.01 cm with four averages in a continuous scan mode. Data were analyzed using software (DCDT) provided by Dr. Walter Stafford (Boston Biomedical Research Institute) to generate a distribution of sedimentation coefficients, $g(s)$, by taking the difference of absorbance profiles at successive times averaged over many differences (Stafford, 1992a,b). The weight average sedimentation coefficients were determined by dividing $\int s \times g(s)\, ds$ by $\int g(s)\, ds$ and then corrected to standard conditions to give $\bar{s}_{20,w}$ (Laue et al., 1992). The integration was done numerically with Origin 3.5.

Curve Fitting. The [^{3}H]vinblastine binding data were plotted as r, bound drug/macromolecule, vs free vinblastine. The sedimentation data were plotted as weight average $\bar{s}_{20,w}$ vs free drug. Total protein concentration in the plateau was determined from $\int g(s)\, ds$. Binding data and sedimentation data were fit using various models for ligand-linked self-association, including isodesmic ligand-mediated, isodesmic ligand-facilitated, or isodesmic ligand-mediated plus ligand-facilitated models (also referred to as the combined model) as described by Na and Timasheff (1985, 1986a). These models involve two or four association constants:

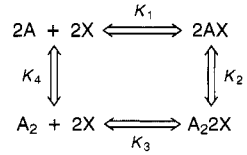

where, in the ligand-mediated model, tubulin heterodimer, A, binds the ligand, X, with an association constant K_1, and two liganded macromolecules, AX, associate with an affinity K_2. For indefinite isodesmic self-association, K_2 is identical for each successive association step (Na & Timasheff, 1980a). In the ligand-facilitated model, the self-association of two unliganded heterodimers, K_4, precedes ligand binding, K_3. The ligand-mediated plus ligand-facilitated model includes all four constants. By microscopic reversibility, $K_1K_2 = K_3K_4$, and thus only three constants can be determined independently. Fitting to these models is based upon Gilbert theory (Gilbert, 1959), as described in Na and Timasheff (1985), and for simplicity assumes a spherical relationship for all polymers, $S_i = (i)^{2/3}S_1$. By utilizing the reported dimensions of vinblastine coiled aggregates (Hodgkinson et al., 1992), the effect of prolate-shaped aggregates was investigated. Furthermore, the K_d for tubulin dissociation has been measured and found to range from 2.1×10^{-9} to 8.0×10^{-7} M^{-1}, depending on solution conditions (Shearwin et al., 1994; Sackett & Lippoldt, 1991; Detrich & Williams, 1978). Therefore, the importance of heterodimer dissociation was also investigated. The nonlinear least-squares program Fitall (MTR Software, Toronto, Canada) was modified to include the appropriate fitting functions and thus obtain the appropriate binding constants (see Results and Discussion). The algorithms developed allow for the global fitting of data sets at multiple tubulin concentrations.

Electron Microscopy. Electron microscopic examination of negatively stained specimens was carried out to examine the morphology of the polymeric products produced under microtubule assembly conditions. Since elution of $\alpha\beta$III-tubulin requires about 4 h from thawing the initial protein to beginning sedimentation experiments, unfractionated tubulin (1 μM) was left on ice for 4 h prior to making samples for electron microscopy. Purified $\alpha\beta$III-tubulin or unfractionated tubulin samples (1 μM) in 100 mM Pipes, 2 mM EGTA, 1 mM GTP, 3 μM taxol, and 1 or 5 mM $MgSO_4$ were warmed at 37 °C for 45 min, diluted 1:1 with fresh 2% glutaraldehyde, and left at room temperature for 1 min. Copper grids (75 mesh, Polysciences, Inc.) were prepared with 0.25% (w/v) polyvinyl formal solution in ethylene dioxide and carbon-coated. Grids were laid on top of 5 μL drops of tubulin/glutaraldehyde solutions for 1 min and then washed with 2 drops of water and negatively stained for 3−5 min with 1% uranyl acetate. Grids were examined and photographed using a Zeiss EM 10 electron microscope.

RESULTS

Sedimentation Velocity Experiments. The association of 2 μM unfractionated tubulin in the presence of vinblastine ranging from 0.05 to 70 μM and 50 μM GDP or 50 μM GTP was studied by sedimentation velocity at 24.6 °C. Figure 1 shows sedimentation coefficient distributions, $g(s)$, calculated from the sedimenting boundary (Stafford, 1992a,b). From the $g(s)$ plots, weight average $\bar{s}_{20,w}$ values were calculated. The inset in Figure 1 shows a comparison of the $\bar{s}_{20,w}$ data in the presence of GDP or GTP plotted against the free vinblastine concentration. For identical concentrations of drug, the sedimentation coefficients are significantly larger in the presence of GDP (Figure 1B) compared to GTP (Figure 1A). Similar experiments were carried out with 1 and 4 μM tubulin in the presence of 50 μM GDP. Figure 2A shows $\bar{s}_{20,w}$ values for unfractionated tubulin at 1, 2, and 4 μM at 24.6 °C plotted against free vinblastine concentrations. The best unconstrained fits for these data using the ligand-mediated plus ligand-facilitated model (combined model) are shown. The parameters obtained from these fits are given in the legend of Figure 2. The values for K_4, the constant for association of unliganded heterodimers, ranged from 2.8×10^4 to 2.7×10^5 M^{-1}. As discussed by Na and Timasheff (1986b), it is not possible to determine all four parameters with certainty due to the high degree of correlation. In fact, these authors suggest that K_4 is less than 2 ×

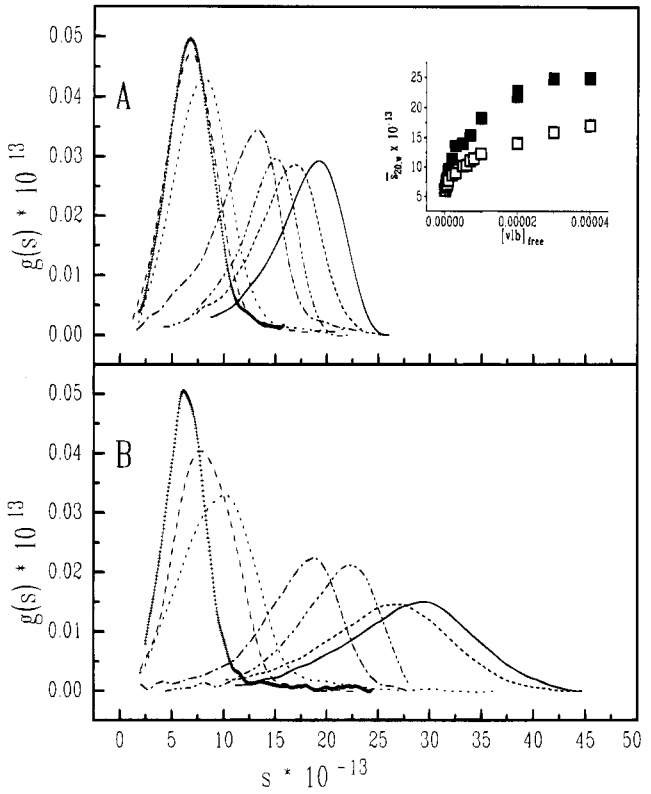

FIGURE 1: Sedimentation coefficient distribution, $g(s)$, plots at increasing vinblastine concentrations at 24.6 °C. (A) $g(s)$ plots of tubulin in the presence of 50 μM GTP. (B) $g(s)$ plots of tubulin in the presence of 50 μM GDP. Velocity sedimentation experiments were carried out as described in Materials and Methods with tubulin (2 μM) and free vinblastine concentrations of 0 (+), 0.5 (— —), 2 (• • •), 7 (-• -•), 11 (-• •-), 30 (- - -), or 40 (—) μM. The inset shows a comparison of the $\bar{s}_{20,w}$ values determined from the $g(s)$ plots as described in Materials and Methods plotted against free vinblastine concentrations [GDP (■) and GTP (□)].

10^3 M^{-1}, although their data could also be described by larger K_4 values. Because four parameters are underdetermined for these data, and a range of K_4 values is consistent with the data, we chose to fix K_4 at 1×10^4 M^{-1}.[2] Below 1×10^4 M^{-1}, the fit and the magnitudes of K_1 and K_2 are insensitive to the magnitude of K_4, although K_3 must adjust accordingly. These data are presented in Table 1. Nearly identical fits were also obtained with the ligand-mediated model (Table 1). A global fit of the data in Figure 2A, using the ligand-mediated model, gave $K_1 = 1.2 \times 10^5$ M^{-1} and $K_2 = 1.7 \times 10^7$ M^{-1}. We were unable to obtain a global fit using the combined model.

The effects of temperature on vinblastine-induced self-association are shown in Figure 3. Sedimentation velocity experiments were carried out with tubulin in the presence of GTP (Figure 3A) or GDP (Figure 3B) and vinblastine concentrations ranging from 0.05 to 70 μM. Sedimentation coefficients at 5, 24.6, and 35.5 °C were plotted against free

[2] Note that while this value of K_4 is consistent with the data, it is somewhat arbitrary. If K_4 is not constrained in fitting the data, the standard deviations of the fits are slightly smaller, consistent with a better fit (compare Figure 2 legend and Table 1). However, the higher values of K_4 obtained by unconstrained fitting of the data are unlikely to be correct because unliganded tubulin has not been found to self-associate even at higher concentrations (Na & Timasheff, 1986b). We found that any value of K_4 between 10 and 1×10^4 M^{-1} resulted in fits with nearly identical standard deviations; therefore, 1×10^4 M^{-1} was chosen as the upper limit for K_4.

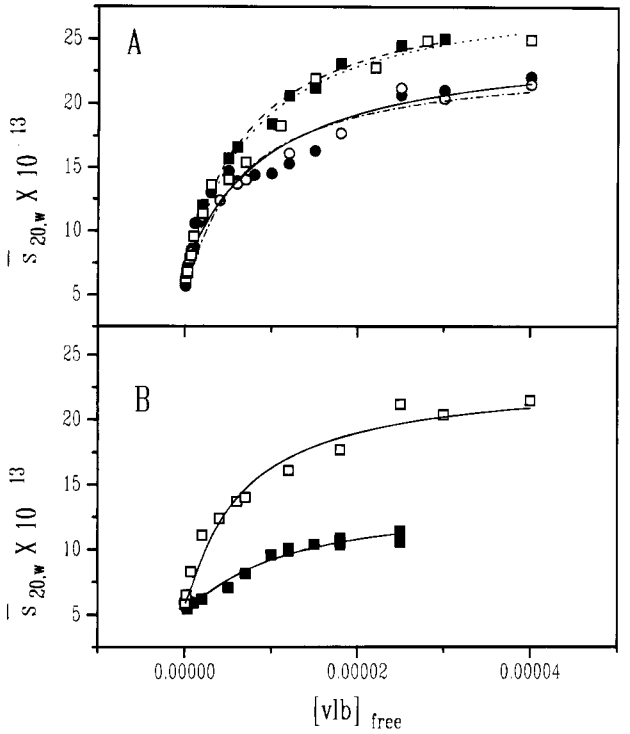

FIGURE 2: Plots of $\bar{s}_{20,w}$ values vs free vinblastine for αβIII-tubulin and unfractionated tubulin at 24.6 °C. (A) Unfractionated tubulin in the presence of 50 μM GDP at 1 (○), 2 (□) or 4 μM (■) and 1 μM αβIII-tubulin (●). The best fits for the data are represented as follows: 1 (— - —), 2 (• • •), or 4 μM (— —) unfractionated tubulin and 1 μM αβIII-tubulin (—). (B) αβIII-Tubulin (1 μM) in the presence of 50 μM GDP (□) or 50 μM GTP (■). The solid lines represent the best fit of each data set independently using the ligand-mediated plus ligand-facilitated model. The K_a values (M^{-1}) for the best fits are as follows: 1 μM, $K_1 = 8.3 \times 10^4$, $K_2 = 2.7 \times 10^6$, $K_3 = 8.2 \times 10^5$, $K_4 = 2.7 \times 10^5$, standard deviation = 1.34; 2 μM, $K_1 = 1.1 \times 10^5$, $K_2 = 9.6 \times 10^5$, $K_3 = 2.7 \times 10^6$, $K_4 = 3.7 \times 10^4$, standard deviation = 0.66; 4 μM, $K_1 = 1.1 \times 10^5$, $K_2 = 5.4 \times 10^5$, $K_3 = 2.1 \times 10^6$, $K_4 = 2.8 \times 10^4$, standard deviation = 0.53.

drug concentrations, and the best fits were determined by using the combined ligand-mediated plus ligand-facilitated model. This resulted in values for K_4 that ranged from 4×10^4 to 3×10^5 M^{-1}. As discussed earlier, all four constants cannot be determined with certainty. It was, therefore, necessary to fix K_4 at 1×10^4 M^{-1}. Table 1 gives the parameters obtained by these fits. The binding constants obtained by fitting with the ligand-mediated model are also summarized in Table 1. Nearly identical fits, as judged by the standard deviations, were obtained by using the ligand-mediated model alone (data not shown). The data and fitted parameters for both models are presented to facilitate comparisons with the published data of Na and Timasheff (1986a,b).

Comparing parameters obtained from fits of GTP and GDP data (2 μM, 24.6 °C), we find no significant difference in K_1, corresponding to the binding of vinblastine to heterodimers. The single exception is the 5 °C data set. For all other data sets, the K_1 values estimated for either the combined or the ligand-mediated model are identical in the presence of GTP or GDP. Thus, even though the vinblastine binding site is located near the exchangeable nucleotide binding site on the β-chain of tubulin (Bai et al., 1990), vinblastine binding is not directly affected by changes in the bound nucleotide. However, the K_2 values, corresponding

Table 1: Equilibrium Constants for the Interaction of Vinblastine with Tubulin[a]

GXP	T (°C)	[TB] (μM)	K_1 (M^{-1})	K_2 (M^{-1})	K_3 (M^{-1})	K_1K_2 (M^{-2})	SD[b]
				PC-Tubulin			
GTP	5.0	2	$3.4 \times 10^4(\pm 1.0)$	$2.0 \times 10^5(\pm 0.04)$	$6.8 \times 10^5(\pm 2.0)$	6.8×10^9	0.82[c]
			$4.7 \times 10^4(\pm 1.0)$	$4.1 \times 10^6(\pm 0.8)$		1.9×10^{11}	0.53[d]
	24.6	2	$1.0 \times 10^5(\pm 0.1)$	$2.3 \times 10^5(\pm 0.01)$	$2.3 \times 10^6(\pm 0.2)$	2.3×10^{10}	0.84[c]
			$1.2 \times 10^5(\pm 0.2)$	$5.1 \times 10^6(\pm 0.6)$		6.1×10^{11}	0.89[d]
	35.5	2	$1.5 \times 10^5(\pm 0.2)$	$2.2 \times 10^5(\pm 0.01)$	$3.3 \times 10^6(\pm 0.2)$	3.3×10^{10}	1.21[c]
			$1.8 \times 10^5(\pm 0.5)$	$4.6 \times 10^6(\pm 0.7)$		8.3×10^{11}	1.23[d]
				βIII-Tubulin			
GTP	24.6	1	$7.4 \times 10^4(\pm 0.8)$	$2.1 \times 10^5(\pm 0.01)$	$1.5 \times 10^6(\pm 0.1)$	1.5×10^{10}	0.41[c]
			$9.2 \times 10^4(\pm 2.0)$	$3.8 \times 10^6(\pm 0.7)$		3.4×10^{11}	0.36[d]
				PC-Tubulin			
GDP	5.0	2	$1.2 \times 10^5(\pm 0.1)$	$3.2 \times 10^5(\pm 0.08)$	$4.0 \times 10^6(\pm 0.3)$	4.0×10^{10}	0.81[c]
			$1.5 \times 10^5(\pm 0.2)$	$1.0 \times 10^7(\pm 0.1)$		1.5×10^{12}	0.95[d]
	24.6	2	$1.2 \times 10^5(\pm 0.01)$	$4.9 \times 10^5(\pm 0.01)$	$5.8 \times 10^6(\pm 0.03)$	5.8×10^{10}	0.72[c]
			$1.3 \times 10^5(\pm 0.1)$	$2.3 \times 10^7(\pm 0.2)$		3.0×10^{12}	0.83[d]
	35.5	2	$1.5 \times 10^5(\pm 0.3)$	$4.4 \times 10^5(\pm 0.03)$	$6.4 \times 10^6(\pm 0.9)$	6.4×10^{10}	2.38[c]
			$1.6 \times 10^5(\pm 0.5)$	$1.8 \times 10^7(\pm 0.5)$		2.9×10^{12}	2.27[d]
	24.6	1	$1.6 \times 10^5(\pm 0.1)$	$4.4 \times 10^5(\pm 0.1)$	$7.0 \times 10^6(\pm 0.3)$	7.0×10^{10}	1.56[c]
			$1.9 \times 10^5(\pm 0.2)$	$1.8 \times 10^7(\pm 0.3)$		3.4×10^{12}	1.58[d]
	24.6	4	$1.3 \times 10^5(\pm 0.03)$	$3.1 \times 10^5(\pm 0.2)$	$3.9 \times 10^6(\pm 0.05)$	3.9×10^{10}	0.58[c]
			$1.6 \times 10^5(\pm 0.2)$	$8.9 \times 10^6(\pm 0.8)$		1.4×10^{12}	0.72[d]
				βIII-Tubulin			
GDP	24.6	1	$1.3 \times 10^5(\pm 0.1)$	$4.4 \times 10^5(\pm 0.02)$	$5.6 \times 10^6(\pm 0.5)$	5.6×10^{10}	1.06[c]
			$1.4 \times 10^5(\pm 0.3)$	$1.9 \times 10^7(\pm 0.3)$		2.7×10^{12}	1.09[d]
				[^{3}H]Vinblastine Binding Data			
GTP	5.0	2	$4.5 \times 10^5(\pm 0.4)$	3.5×10^5	$2.6 \times 10^7(\pm 8.6)$	1.6×10^{11}	0.18[e]
			$4.5 \times 10^5(\pm 0.8)$	4.1×10^6		1.9×10^{12}	0.63[f]
GDP	5.0	2	$4.0 \times 10^5(\pm 0.5)$	5.0×10^5	$5.2 \times 10^7(\pm 0.3)$	2.0×10^{11}	0.19[e]
			$4.8 \times 10^5(\pm 0.8)$	1.0×10^7		4.8×10^{12}	0.58[g]
				Na and Timasheff (1986b)[h]			
GTP	20.0	5−20	3.8×10^5	5.2×10^5	4.4×10^9	1.98×10^{11}	

[a] Fitting of $\bar{s}_{20,w}$ data to either an indefinite ligand-mediated plus ligand-facilitated self-association model or to an indefinite ligand-mediated self-association model. Note that the first line for each solution condition is the combined model fit and the second line is the ligand-mediated fit. [b] Standard deviation of the fit in units of S or r. [c] Fit with the complete indefinite ligand-mediated plus ligand-facilitated self-association model; $K_4 = 1 \times 10^4$ M^{-1}. [d] Fit with the indefinite ligand-mediated self-association model. [e] Fit with the combined ligand-mediated plus ligand-facilitated model; an additional parameter K_0 corresponding to two weak vinblastine binding sites not linked to self-association is included in these fits. $K_0 = 5 \times 10^3$ M^{-1} and $K_4 = 5.5 \times 10^3$ M^{-1} for GTP and 3.6×10^3 M^{-1} for GDP. [f] Fit with the ligand-mediated model; K_0 constrained to 3.0×10^4 M^{-1}. [g] Fit with the ligand-mediated model; K_0 constrained to 1.1×10^4 M^{-1}. [h] Na and Timasheff (1986b); ligand-mediated plus ligand-facilitated model.

Table 2: Thermodynamic Parameters for Vinblastine−Tubulin Interaction at 24.6 °C

	K_1K_2 (M^{-2})	$\Delta G°$ (kcal/mol)	$\Delta S°$ (cal/mol·K)	$\Delta H°$ (kcal/mol)
		Ligand-Mediated plus Ligand-Facilitated Model		
GTP	2.3×10^{10}	−14.1	77	8.7
GDP	5.8×10^{10}	−14.7	58	2.5
		Ligand-Mediated Model		
GTP	6.1×10^{11}	−16.1	68	4.2
GDP	3.0×10^{12}	−17.0	64	2.0

to the association of liganded heterodimer, are drastically different for GTP− and GDP−tubulin. For the combined model, the value of K_2 for GDP−tubulin is approximately 2-fold larger than that for GTP−tubulin, while for the ligand-mediated model, K_2 increases nearly 4-fold in the presence of GDP. This increase in K_2 is seen in all cases for either model and thus is considered to be highly reliable, although the magnitude of this difference is model-dependent. Thus, there is a 2−4-fold enhancement in K_2, indicating an effect primarily on tubulin self-association that is caused by the presence of GDP.

The observed vinblastine-induced association of tubulin was enhanced by raising the temperature. At all temperatures, K_1K_2 is larger in the presence of GDP than GTP. The inset in Figure 3 shows a van't Hoff plot of these data. van't Hoff analysis of K_1 or K_2 alone could not be used to obtain reliable thermodynamic results. Table 2 gives the estimated thermodynamic parameters for the overall process. The ΔH_{app} is more positive for ligand-induced self-association in the presence of GTP compared to GDP. For the combined model, ΔH_{app} is 8.7 and 2.5 kcal/mol for the GTP and GDP data, respectively. For the ligand-mediated model, the estimated values are 4.2 and 2.0 kcal/mol, respectively. Thus, although the absolute values are model-dependent, the trend is the same. The reduced enthalpy in the presence of GDP results in an increased overall free energy and a larger extent of ligand-induced association at any given temperature.

[^{3}H]Vinblastine Binding to Tubulin. In order to validate our results from sedimentation experiments and better compare them with the binding data reported by others (Na & Timasheff, 1986b; Singer et al., 1988), ultrafiltration using an Amicon micropartition system was used to study the binding of [^{3}H]vinblastine to 2 μM tubulin at 5 °C. The concentrations of vinblastine ranged from 0.05 to 50 μM. Figure 4 shows a comparison of drug binding data in the presence of GDP (Figure 4A) and GTP (Figure 4B). Bound vinblastine per tubulin heterodimer (μM/μM) is plotted against free drug. Nonlinear least-squares fitting of the data using the isodesmic ligand-mediated plus ligand-facilitated model (Na & Timesheff, 1986b) gave the parameters shown

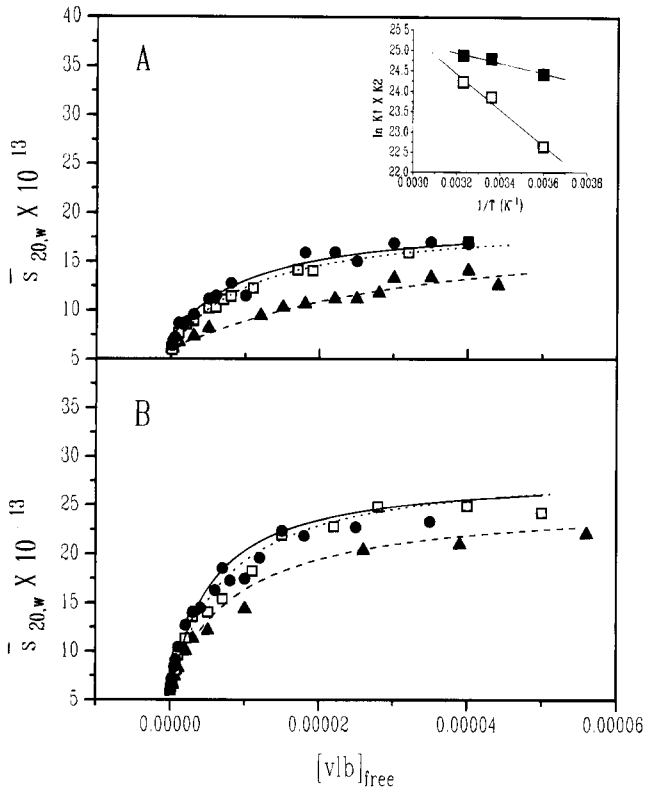

FIGURE 3: Combined ligand-mediated plus ligand-facilitated fits of temperature data: plots of $\bar{s}_{20,w}$ values vs free vinblastine obtained at 5 (▲), 24.6 (□), or 35.5 (●) °C. The lines represent the best fit of the data at 5 (— —), 24.6 (•••), or 35.5 (—) °C, using the combined ligand-mediated plus ligand-facilitated model. (A) Tubulin (2 μM) in the presence of 50 μM GTP. The best fit gave the following parameters (M^{-1}): 5 °C, $K_1 = 2.43 \times 10^4$, $K_2 = 5.16 \times 10^5$, $K_3 = 2.94 \times 10^4$, $K_4 = 4.27 \times 10^4$, standard deviation = 0.37; 24.6 °C, $K_1 = 7.80 \times 10^4$, $K_2 = 5.38 \times 10^5$, $K_3 = 8.56 \times 10^5$, $K_4 = 4.90 \times 10^4$, standard deviation = 0.76; 35.5 °C, $K_1 = 7.76 \times 10^4$, $K_2 = 9.93 \times 10^5$, $K_3 = 4.77 \times 10^5$, $K_4 = 1.62 \times 10^5$, standard deviation = 1.04. (B) Tubulin (2 μM) in the presence of 50 μM GDP. The best fits gave the following parameters (M^{-1}): 5 °C, $K_1 = 8.51 \times 10^4$, $K_2 = 9.98 \times 10^5$, $K_3 = 1.06 \times 10^6$, $K_4 = 8.03 \times 10^4$, standard deviation = 0.51; 24.6 °C, $K_1 = 1.05 \times 10^5$, $K_2 = 9.59 \times 10^5$, $K_3 = 2.72 \times 10^6$, $K_4 = 3.68 \times 10^4$, standard deviation = 0.66; 35.5 °C, $K_1 = 1.46 \times 10^5$, $K_2 = 4.35 \times 10^5$, $K_3 = 6.35 \times 10^6$, $K_4 = 1 \times 10^4$, standard deviation = 2.38. It was necessary to constrain K_4 to 1×10^4 M^{-1} in order to obtain these parameters for the 35.5 °C data, otherwise K_4 approached zero without reaching an acceptable fit of the data. The binding constants obtained when K_4 was constrained to 1×10^4 M^{-1} are given in Table 1. The inset shows a van't Hoff plot of the overall affinity, K_1K_2, in the presence of GTP (□) or GDP (■). The thermodynamic parameters are summarized in Table 2.

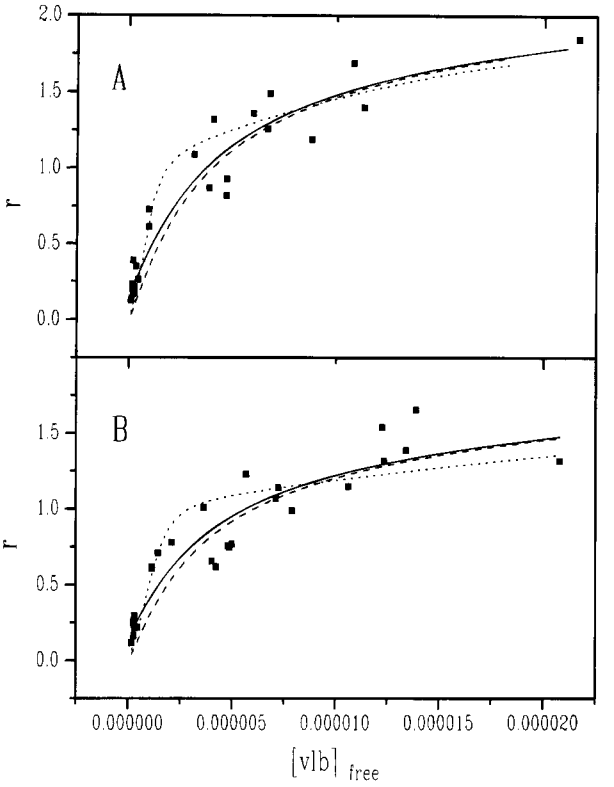

FIGURE 4: [^{3}H]Vinblastine binding data fit with the combined ligand-mediated plus ligand-facilitated model or ligand-mediated model. Experiments were carried out on ice as described in Materials and Methods. Nonlinear least-squares fitting was carried out with the combined model while constraining K_0 to 5×10^3 M^{-1} and K_4 to 5×10^2 (— —) or 5×10^4 M^{-1} (—). The values for K_1, K_2, and K_3 were independent of this range of K_4 values. Data were also fit with the ligand-mediated model alone (- -). Parameters obtained from these fits are given in Table 1. (A) Tubulin (2 μM) in the presence of GDP. (B) Tubulin (2 μM) in the presence of GTP.

in Table 1. As discussed earlier, the parameters are underdetermined for these data. We therefore fixed K_0 (the association constant for binding of vinblastine to low-affinity sites) and K_4 and then searched for the best fit at K_2 values ranging from 1×10^5 to 1×10^9 M^{-1}. The value suggested by Na and Timasheff (1986a) for K_0, 5×10^3 M^{-1}, was used. K_4 was fixed at values between 5×10^2 (Figure 4, dashed lines) and 5×10^4 M^{-1} (Figure 4, solid lines), and nearly identical parameters were obtained, regardless of the K_4 value. The binding constants for the association of liganded dimers, K_2, or binding of vinblastine to polymers, K_3, were found to be slightly larger in the presence of GDP compared to GTP, as was the product, K_1K_2 (Table 1). We also attempted to fit the data with the ligand-mediated model alone (Figure 4A,B, dotted line), and the results of this fit are shown in Table 1. The standard deviations of the ligand-mediated fits were significantly higher than those of the combined model fits, consistent with the conclusions of Na and Timasheff (1986a).

It should be noted that the simplest isodesmic model assumes a spherical shape for the polymers. Because this is unlikely to be true, even for the smallest polymers, we also fit the binding data, as well as the sedimentation data, with a model that differed from the combined ligand-mediated plus ligand-facilitated model only in that it assumed a prolate shape for the aggregate (see Materials and Methods). The resulting binding constants were larger, as expected, because the larger frictional coefficient of a nonspherical polymer reduces the sedimentation coefficient, thus requiring a larger extent of polymerization to fit the data. However, the standard deviation for each fit was also larger (data not shown), possibly due to an incorrect functional form of the shape factor.[3] Thus, this approach was not continued. In addition, we investigated the possibility that there may be a significant contribution from the dissociation of the αβ-heterodimer at low tubulin concentra-

[3] Note that the isodesmic assumption has been questioned (Chatelier, 1987; Chatelier & Minton, 1987) on the grounds that the entropy of monomer addition to a polymer is not a constant for all polymer sizes and shapes. Thus, a more correct theory should use an isoenthalpic model and a shape-dependent entropy term for the magnitude of K_2 or K_4 and a shape-dependent frictional coefficient in the fitting function.

tions. We included in the fitting function the reported dissociation constants for GDP− or GTP−tubulin (Shearwin et al., 1994), 2.08×10^{-9} or 1.43×10^{-8} M^{-1}, respectively. We found that these constants resulted in a small increase in the standard deviation of the final fit and, in fact, resulted in slightly larger values of K_1 and K_2 in all cases. We also fit data using the larger K_d values reported by Sackett and Lippoldt (1991) and Detrich and Williams (1978). The resulting fits had even larger standard deviations and larger K_1K_2 values. Thus, we conclude that heterodimer dissociation in the presence of vinblastine is not a significant event in the tubulin concentration range of 1−4 μM. Similar to the effect colchicine has on the stabilization of tubulin heterodimers (Detrich et al., 1982), vinblastine may induce or favor a conformation that dissociates less readily.

The [^{3}H]vinblastine binding experiments were carried out at 0−5 °C and are, therefore, comparable to sedimentation data collected at 5 °C. The experiments with radioactive drug, fit with the ligand-mediated model, showed a 2.5-fold increase in K_1K_2 for the GDP data compared to the GTP data (Table 1). When fit with the combined ligand-mediated plus ligand-facilitated model, this increase is reduced (Table 1). For the sedimentation data at 2 μM tubulin and 5 °C fit with the combined model, K_1K_2 is nearly 6-fold larger in the presence of GDP compared to GTP (Table 1). The same data fit with the ligand-mediated model resulted in a 10-fold larger K_1K_2 for the GDP data than for the GTP data (Table 1). Thus, the binding data are consistent with the sedimentation data, but due to more noise in the data and/or the need to include an additional parameter, K_0, the nucleotide effect is less dramatic. Note that K_0 is uncoupled from self-association and, thus, is not evident in the sedimentation data (Na & Timasheff, 1985). We conclude that sedimentation velocity is preferred as a technique for studying vinblastine−tubulin−nucleotide interactions.

Association of Purified αβIII-Tubulin. In order to investigate the effects of vinblastine on the self-association of an individual isotype, we purified αβIII-tubulin by a novel immunoaffinity chromatography procedure and then studied the association of αβIII-tubulin by analytical ultracentrifugation. Figure 5 shows two Western blots of void protein (the fraction that does not bind) from an anti-βIII affinity column and eluted αβIII-tubulin (the bound fraction) from the same column. The blot in Figure 5A was reacted with βII-specific antibody, 7B9, and the blot in Figure 5B was reacted with βIII-specific antibody, TUJ1. In order to obtain the maximum amount of βIII-tubulin, the column was saturated with tubulin. Nonspecific binding to agarose occurs, as evidenced by the slight reaction of βII with the bound fraction in Figure 5A. In order to estimate the amount of nonspecific binding to the column, void material (free of bound tubulin) was pooled, reloaded on the column, and eluted with 3.5 M potassium iodide. From quantification of the initial and bound fractions, it was estimated that less than 3% of the peptide-eluted protein is nonspecifically bound.

Figure 6 shows a Western blot of an isoelectric focusing gel of unfractionated tubulin and the peptide-eluted αβIII-tubulin. It can be seen that the purified βIII-tubulin is composed of all of the posttranslationally modified forms found in unfractionated tubulin (3−5 bands). The quality of the purified αβIII-tubulin was assayed by polymerization in the presene of taxol, with subsequent electron microscopic observation of the polymers. Figure 7 shows electron micrographs of αβIII-tubulin in the presence of taxol with 1 and 5 mM $MgSO_4$ (Figure 7A,C, respectively) and unfractionated tubulin in the presence of the same amount of taxol and 1 mM $MgSO_4$ (Figure 7B). The formation of microtubules with normal morphology required 5 mM $MgSO_4$ for αβIII-tubulin, compared to 1 mM $MgSO_4$ for unfractionated tubulin. Note that unfractionated tubulin was aged for 4 h on ice to provide the approriate control (see Materials and Methods).

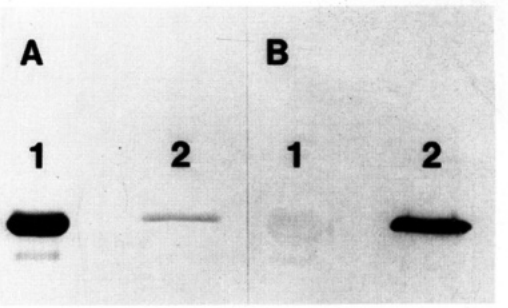

FIGURE 5: Western blots of void protein and bound material from an anti-βIII immunoaffinity column. The anti-βIII immunoaffinity column was loaded with tubulin and eluted as described in Materials and Methods. Aliquots were taken from the void volume and peptide-eluted fractions. SDS−PAGE and Western blotting were carried out as described in Materials and Methods. Lane 1 contains the void fraction and lane 2 contains bound fractions. (A) Western blot reacted with TU7B9, an antibody prepared against the βII peptide. (B) Western blot reacted with TUJ1, an antibody prepared against the βIII peptide. Note that the βII antibody reacts very slightly with the bound material. We determined that this fraction is due to the nonspecific binding of tubulin to agarose and estimate that it represents 3% or less of the total bound fraction (see Results).

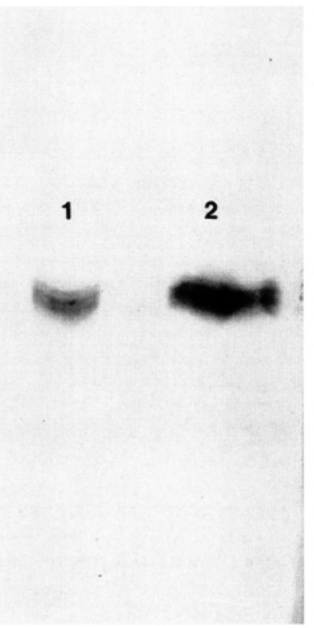

FIGURE 6: Western blot of an isoelectric focusing gel with unfractionated and purified αβIII-tubulin: lane 1, unfractionated tubulin; lane 2, αβIII-tubulin. The filter was reacted with TUJ1, an antibody prepared against the βIII peptide. It can be seen that all bands present in unfractionated tubulin are present in the purified βIII material.

This of course would add additional parameters that cannot be uniquely determined. Thus, we can conclude, on the basis of these considerations, that the overall K_1K_2 values that we estimate with either model are probably underestimates.

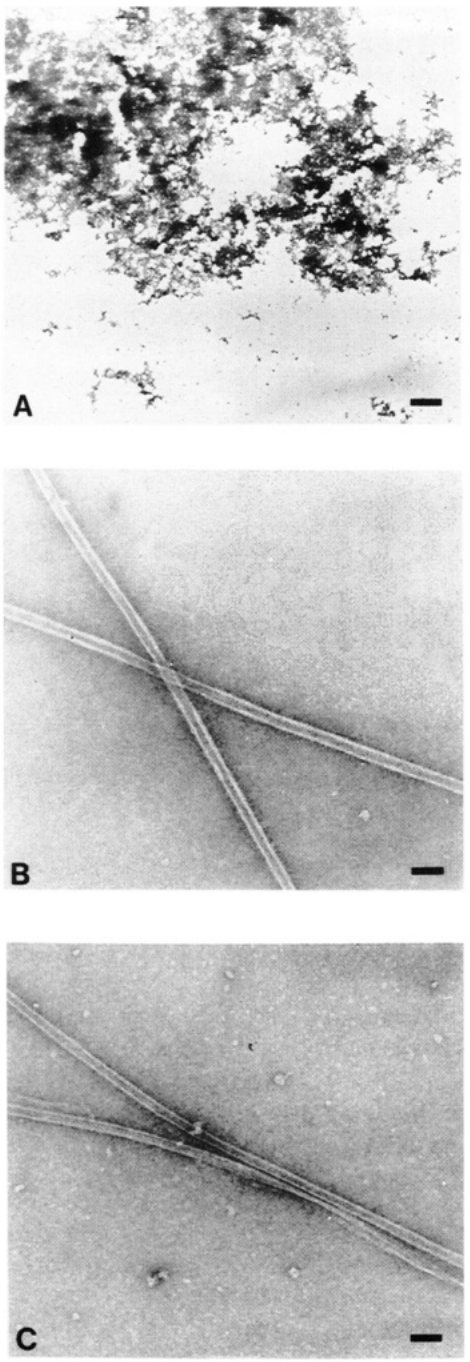

FIGURE 7: Electron micrographs of unfractionated and αβIII-tubulin polymerized with taxol at 37 °C. (A) αβIII-Tubulin (1 μM) in the presence of 3 μM taxol and 1 mM magnesium (bar = 520 nm). (B) Unfractionated tubulin (1 μM) in the presence of 3 μM taxol and 1 mM magnesium (bar = 67 nm). (C) αβIII-Tubulin (1 μM) in the presence of 3 μM taxol and 5 mM magnesium (bar = 70 nm).

Purified αβIII-tubulin (1 μM) at 24.6 °C in the presence of GDP or GTP at vinblastine concentrations ranging from 0.05 to 40 μM was used in sedimentation velocity experiments as described earlier for unfractionated tubulin. Figure 2 shows sedimentation coefficients of αβIII-tubulin plotted against free vinblastine concentrations. In the presence of GDP, αβIII-tubulin and unfractionated tubulin associate to the same extent (Figure 2A). The association constants obtained from fitting the data with the ligand-mediated plus ligand-facilitated model or the ligand-mediated model are shown in Table 1. Within error, there is no difference between unfractionated and αβIII-tubulin in the presence of GDP. A difference in the extent of association, similar to that found between unfractionated tubulin in GDP or GTP buffers, was also found with αβIII-tubulin (Figure 2B). The overall association, K_1K_2, increases 3.7−8.0-fold, while K_2, the association of liganded heterodimer, increases 1.7−5.0-fold, depending on the model used. There is a small nucleotide effect on K_1, the affinity of vinblastine for the tubulin heterodimer, but given the overall results with unfractionated tubulin, this is not likely to be significant. Thus, it appears that vinblastine-induced association of unfractionated and αβIII-tubulin are identical. There is a magnesium dependnce for taxol polymerization of αβIII-tubulin that suggests a difference in microtubule formation between unfractionated and αβIII-tubulin (Figure 7). These results suggest that the energetics of microtubule formation and vinblastine-induced self-association into spirals or coils measure different structure−function relationships or different functional aspects of the tubulin isotypes. This could be due to differences in taxol binding (Lu & Luduena, 1993) or differences in magnesium binding. Since Mg^{2+} will induce tubulin ring formation in the presence of GDP (Howard & Timasheff, 1986), we are currently exploring the Mg^{2+} dependence of ring formation for unfractionated and αβIII-tubulin.

DISCUSSION

Nucleotide Dependence of Vinblastine-Induced Tubulin Self-Association. We have demonstrated here that GDP enhances vinblastine-induced self-association of tubulin. We obtained association constants by fitting sedimentation velocity data with indefinite isodesmic models: ligand-mediated or ligand-mediated plus ligand-facilitated. Both models give nearly identical fits as measured by comparing the standard deviations (Table 1). The products K_1K_2 obtained from data collected in the presence of GDP at 24.6 °C by fitting with the combined or ligand-mediated model were 5.8×10^{10} and 3.0×10^{12} M^{-2}, respectively. The fits for data collected in the presence of GTP at the same temperature gave K_1K_2 values of 2.3×10^{10} and 6.1×10^{11} M^{-2} for the combined and ligand-mediated models, respectively. Thus, regardless of the model used in the fitting function, GDP was found to enhance tubulin self-association. These binding constants are consistent with the values reported by Na and Timasheff (1986b) for ligand-mediated plus ligand-facilitated fits of batch gel filtration data from experiments with [^{3}H]vinblastine at 20 °C in 10 mM sodium phosphate (pH 7.0), 1 mM Mg^{2+}, and 0.1 mM GTP, where they estimated K_1K_2 to be 1.98×10^{11} M^{-2}. Our somewhat smaller value, 2.3×10^{10} M^{-2}, for sedimentation data in the presence of GTP, fit with the combined model, is most likely due to the inclusion of two additional low-affinity sites in the [^{3}H]vinblastine binding data and, thus, a propagation of error or bias into the other fitted parameters. Note that our [^{3}H]vinblastine binding data, at 5 °C fit with the combined model, is in good agreement with the overall affinity reported by Na and Timasheff (1986b), 1.6×10^{11} vs 1.98×10^{11} M^{-2}, respectively (Table 1).

A further comparison of the binding constants reported here (Table 1) shows that the product K_1K_2 is 10−50-fold larger when the sedimentation or binding data are fit with the ligand-mediated model than with the combined model. For example, at 24.6 °C in the presence of GTP, K_1K_2 was estimated to be 6.1×10^{11} and 2.3×10^{10} M^{-2} for the ligand-

mediated and combined models, respectively. K_1 is essentially unchanged, 1.2×10^5 and 1.0×10^5 M^{-1}, for the ligand-mediated and combined models. Similarly, when we fit micropartition data obtained in the presence of GTP, using [^{3}H]vinblastine at 5 °C with the ligand-mediated or combined model, we obtained K_1K_2 values of 1.9×10^{12} and 1.6×10^{11} M^{-2}. Again, K_1 values are identical, 4.5×10^5 M^{-1}, for both fits. Thus, the difference in the two sets of parameters is due to an increase in K_2. For any given data set, K_2 and the product K_1K_2 vary depending on the model. What is the origin of this model-dependent variation? First of all, it should be noted that our experiments were carried out at very low protein concentrations, 1−4 μM, compared to 10−200 μM for similar experiments by other investigators (Na & Timasheff, 1986b; Singer et al., 1988). Since the ligand-mediated model is a reasonable description of the sedimentation data presented in this study (Table 1), it is unlikely that there is a significant contribution from the association of unliganded heterodimers, K_4, at the lower concentrations. Secondly, in the ligand-mediated case, only liganded heterodimers can associate, and thus, there is no alternate path to association. This effectively means that $K_4 = 0$, an assumption that actually violates microscopic reversibility. Thus, K_2 must increase in the ligand-mediated model to compensate for the loss of an alternate path. Note that a good fit of the data with the ligand-mediated model implies that the ligand-facilitated path is kinetically excluded, possibly because the polymers formed by K_4, the self-association of unliganded heterodimers, must undergo a slow conformational change to bind drug. Finally, as stated earlier, the spherical approximation to the sedimentation coefficients of the polymers reduces the overall equilibrium values estimated. The combined model probably underestimates the overall energetics of the reaction, and the ligand-mediated fit is probably a better estimate of the overall equilibrium or total energetics of the process.

In summary, we found that sedimentation coefficients obtained in the presence of GDP are larger than those obtained in the presence of GTP. K_1, binding of vinblastine to heterodimers, in general is not nucleotide-dependent; however, K_2, association of liganded heterodimers, is 2−4-fold larger in the presence of GDP compared to GTP. This difference is reflected in the thermodynamic parameters determined from sedimentation data at 5, 24.6, and 35.5 °C. ΔH_{app} determined from the ligand-mediated fit for data collected in the presence of GDP was 2.0 kcal/mol, compared to 4.2 kcal/mol for the GTP data. GDP lowers the ΔH_{app} (Table 2), and this results in a more negative ΔG for tubulin self-association. The absolute value of this enthalpy change is model-dependent and coupled to the corresponding entropy change. Thus, it is not possible to make any detailed statements about the mechanism of this nucleotide effect on the thermodynamic parameters. We can only conclude that overall self-association is favored by GDP, and the maximum sedimentation coefficients are found to be larger in the presence of GDP, 25S, than in the presence of GTP, 18S. Note that, consistent with previous work, the overall driving force is entropic (Na & Timasheff, 1980b).

Figure 8 summarizes the overall thermodynamic parameters as a Weber plot (Weber, 1975). For the ligand-mediated model, the overall free energy is $\Delta G_1° + \Delta G_2°$, where $\Delta G_1°$ is the free energy of vinblastine binding to the heterodimer and $\Delta G_2°$ is the free energy of association of

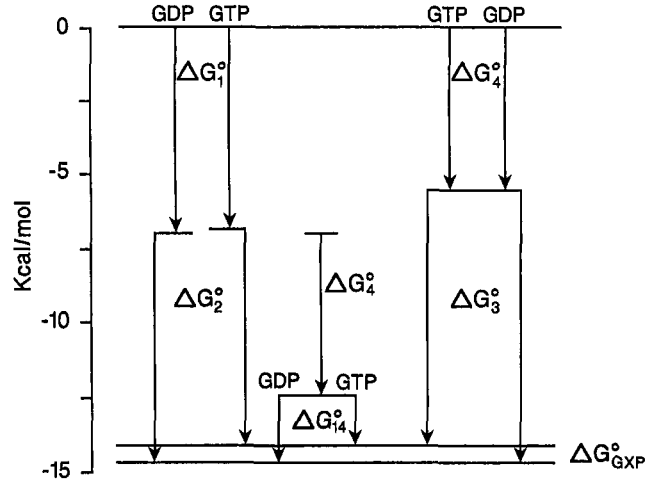

FIGURE 8: Weber plot (Weber, 1975) or the free energy linkage between vinblastine binding and indefinite self-association of tubulin. Vinblastine binding $\Delta G_1°$ enhances self-association such that $\Delta G_2° > \Delta G_4°$. By the linkage relationship, self-association enhances vinblastine binding such that $\Delta G_3° > \Delta G_1°$. The linkage free energy $\Delta G_{14}° = \Delta G_2° - \Delta G_4° = \Delta G_3° - \Delta G_1°$. In addition, the linkage free energy in the presence of GDP is greater than that in the presence of GTP. This corresponds to an additional linkage free energy, $\Delta G°_{gxp}$, that is manifested in $\Delta G_2°$ or $\Delta G_3°$ in the presence of GDP.

liganded heterodimers, corresponding to K_1 and K_2 in the reaction scheme, respectively. It is clear that, for the combined model, $\Delta G_1° + \Delta G_2° = \Delta G_3° + \Delta G_4°$, where $\Delta G_3°$ is the free energy for binding of vinblastine to polymers and $\Delta G_4°$ represents free energy for association of unliganded heterodimers. Vinblastine binding, $\Delta G_1°$, enhances self-association such that $\Delta G_2° > G_4°$, while self-association, $\Delta G_4°$, enhances vinblastine binding such that $\Delta G_3° > \Delta G_1°$. The linkage free energy, $\Delta G_{14}° = \Delta G_2° - \Delta G_4° = \Delta G_3° - \Delta G_1°$, corresponds to the magnitude of free energy enhancement. For the sedimentation data alone, this value is larger when GDP is present (2.18 ± 0.14 kcal/mol) than GTP (1.79 ± 0.10 kcal/mol). The difference in these values, $\Delta G°_{gxp}$, is the free energy enhancement caused by GDP vs GTP binding to tubulin. When sedimentation data are fit with the combined model, $\Delta G°_{gxp}$ is 0.39 kcal/mol, but if both models are included in the calculation, it is somewhat larger, 0.85 ± 0.28 kcal/mol. Thus, while the magnitude of the nucleotide effect is model-dependent there is a relative difference in the linkage of GDP vs GTP binding and vinblastine-induced self-association of tubulin.

Vinblastine-Induced Association of αβIII-Tubulin. We carried out sedimentation velocity experiments with purified αβIII-tubulin in an effort to determine whether vinblastine interacts preferentially with this isotype. We observed identical parameters for vinblastine-induced self-association and the same GDP enhancement of self-association that occurs with unfractionated tubulin in the presence of the drug. This is not in agreement with the results of Khan and Luduena (1993), who report significant differences in the interaction of βIII-tubulin and other isotypes with vinblastine. However, they used an inhibition of microtubule polymerization assay to study the interaction of vinblastine with tubulin isotypes in the presence of MAPs. Our results indicate that there is a magnesium dependence for taxol polymerization of αβIII-tubulin that does not occur with unfractionated tubulin (Figure 7). We found that βIII-tubulin requires increased Mg^{2+} to form taxol-stabilized microtu-

bules. Since vinblastine binding and vinblastine-induced self-association of the purified isotype are identical to those of unfractionated tubulin, we suggest that the results of Khan and Luduena (1993) may be due to differences in the energetics of microtubule formation and not in the interaction with vinblastine.

Implications for the Interaction of Vinblastine with Microtubules. The enhancement of vinblastine−tubulin interactions by GDP may have important consequences for the mechanism of substoichiometric stabilization of microtubules that has been reported for vinblastine (Jordan & Wilson, 1990; Toso et al., 1993). The mode of interaction is hypothesized to be at the ends of microtubules. A vinblastine-induced spiral is envisaged to be growing from a protofilament at the GTP cap. Since GDP−tubulin spirals interact with vinblastine with higher affinity (K_3 = (4−7) × 10^6 M^{-1}; see Table 1), spirals could also emanate from the GDP core. As demonstrated in our thermodynamic analysis, drug binding enhances spiral formation, and spiral formation enhances drug binding. Thus, propagation of the spiral would enhance drug binding to the microtubule core−cap interface. Spiral formation is a conformational change that disrupts interactions between protofilaments in the microtubule body and may enhance vinblastine binding by exposing the vinblastine binding sites, although energetic considerations do not require this. At low drug concentrations, addition of liganded subunits to the dissociating end of a microtubule may stabilize the polymer. Growth could be inhibited because unliganded subunits do not readily add to spirals. At higher drug concentrations, extensive propagation of the spiral into the GDP−tubulin core could lead to destabilization of the entire microtubule and disassembly into vinblastine polymers. The higher affinity of vinblastine for GDP−tubulin spirals, K_3 in our mechanism, is consistent with this propagation mechanism. A previous estimate of the affinity of vinblastine for microtubule ends was 5.3 × 10^5 M^{-1} (K_d = 1.9 μM; Wilson et al., 1982). While this is nearly an order of magnitude smaller than the K_3 values we report here, (2.0−3.0) × 10^6 M^{-1} for GTP−tubulin and (4.0−7.0) × 10^6 M^{-1} for GDP−tubulin, it suggests that the proposed mechanism is reasonable. Direct binding of vinblastine to the microtubule core may be unfavorable dur to steric hindrance. The vinblastine binding site is located near the GTP binding site and, like the GTP binding site, may be buried in the lattice and thus inaccessible. Alternatively, the energetic cost of forming a spiral directly in the microtubule body may be too great, due to the disruption of protofilament− protofilament interactions, and thus lead to reduced affinity for the microtubule body. This would favor vinblastine binding to the ends, where spiral propagation could occur one subunit at a time.

Taxol also stabilizes microtubules. However, at substoichiometric concentrations, taxol appears to selectively bind to the microtubule core, with reduced affinity for the microtubule ends (Derry et al., 1995). Thus taxol stabilizes the microtubule lattice, although it may favor a slightly alternate structure (Andreu et al., 1992), while vinblastine favors a spiral polymer that necessarily disrupts the microtubule lattice. These considerations appear to account for the differences in the modes of action of taxol and vinblastine. It is not clear whether similar mechanisms would apply to the stabilization of microtubules by substoichiometric concentrations of podophyllotoxin, since podophyllotoxin does not induce polymer formation of any kind (Schilstra et al., 1989). However, a similar mechanism may explain the interaction of the tubulin−colchicine complex with dynamic microtubules, since colchicine is known to disrupt the lattice into an alternate polymer form (Vandcandelaere et al., 1994).

ACKNOWLEDGMENT

We thank Alex Slawson and Sandor Varadi for technical assistance with these experiments. We are grateful to Dr. Matthew Suffness of the National Cancer Institute for supplying taxol and to Pelahatchie Country Meat Packers for providing pig heads for tubulin purification.

REFERENCES

Andreu, J. M., Bordas, J., Diaz, J. F., Garcia de Ancos, J., Gil, R., Medrano, F. J., Nogales, E., Pantos, E., & Towns-Andrews, E. (1992) *J. Mol. Biol. 226*, 169−184.
Bai, R., Petit, G., & Hamel, E. (1990) *J. Biol. Chem. 265*, 17141−17149.
Bradford, M. M. (1976) *Anal. Biochem. 72*, 248−254.
Chatelier, R. C. (1987) *Biophys. Chem. 28*, 121−128.
Chatelier, R. C., & Minton, A. P. (1987) *Biopolymers 26*, 507−524.
Correia, J. J., Baty, L. T., & Williams, R. C., Jr. (1987) *J. Biol. Chem. 262*, 17278−17284.
Derry, W. B., Wilson, L., & Jordan, M. A. (1995) *Biochemistry 34*, 2203−2211.
Detrich, H. W., & Williams, R. C., Jr. (1978) *Biochemistry 17*, 3900−3907.
Detrich, H. W., Williams, R. C., Jr., & Wilson, L. (1982) *Biochemistry 21*, 2392−2400.
Frigon, R. P., & Timasheff, S. N. (1975a) *Biochemistry 14*, 4559−4566.
Frigon, R. P., & Timasheff, S. N. (1975b) *Biochemistry 14*, 4567−4573.
Gilbert, G. A. (1959) *Proc. R. Soc. London, Ser. A 250*, 377−388.
Himes, R. H. (1991) *Pharmacol. Ther. 51*, 257−267.
Hodgkinson, J. L., Hutton, T., Medrano, F. J., & Bordas, J. (1992) *J. Struct. Biol. 109*, 28−38.
Howard, W. D., & Timasheff, S. N. (1986) *Biochemistry 25*, 8292−8300.
Jordan, M. A., & Wilson, L. (1990) *Biochemistry 29*, 2730−2739.
Jordan, M. A., Thrower, D., & Wilson, L. (1991) *Cancer Res. 51*, 2212−2222.
Khan, I. A., & Luduena, R. F. (1993) *Mol. Biol. Cell 4* (supplement), 264a.
Laue, T. M., Shah, B. D., Ridgeway, T. M., & Pelletier, S. L. (1992) in *Analytical Ultracentrifugation in Biochemistry and Polymer Science* (Harding, S. E., Rowe, A. J., & Horton, J. C., Eds.) pp 90−125, The Royal Society of Chemistry, Cambridge, UK.
Lee, J. C., Harrison, D., & Timasheff, S. N. (1975) *J. Biol. Chem. 250*, 9276−9282.
Lee, M. K., Tuttle, J. B., Rebhun, L. I., Cleveland, D. W., & Frankfurter, A. (1990) *Cell Motil. Cytoskeleton 17*, 118−132.
Liu, S., & Stafford, W. F., III (1995) *Anal. Biochem. 224*, 199−202.
Lobert, S., & Correia, J. J. (1994) *Electrophoresis 15*, 930−931.
Lu, Q., & Luduena, R. F. (1993) *Cell Struct. Funct. 18*, 173−182.
Na, G. C., & Timasheff, S. N. (1980a) *Biochemistry 19*, 1347−1354.
Na, G. C., & Timasheff, S. N. (1980b) *Biochemistry 19*, 1355−1365.
Na, G. C., & Timasheff, S. N. (1985) in *Methods in Enzymology* (Hirs, C. H. W., & Timasheff, S. N., Eds.) Vol. 117, pp 459−495, Academic Press, New York.
Na, G. C., & Timasheff, S. N. (1986a) *Biochemistry 25*, 6214−6222.
Na, G. C., & Timasheff, S. N. (1986b) *Biochemistry 25*, 6222−6228.
Sackett, D. L., & Lippoldt, R. E. (1991) *Biochemistry 30*, 3511−3517.

Schilstra, M. J., Martin, S. R., & Bayley, P. M. (1989) *J. Biol. Chem. 264*, 8827−8834.
Shearwin, K. E., Perez-Ramirez, B., & Timasheff, S. N. (1994) *Biochemistry 33*, 885−893.
Singer, W. D., Hersh, R. T., & Himes, R. H. (1988) *Biochem. Pharmacol. 37*, 2691−2696.
Sophianopoulos, J. A., Durham, S. J., Sophianopoulos, A. J., Ragsdale, H. L., & Cropper, W. P. (1978) *Arch. Biochem. Biophys. 187*, 132−137.
Stafford, W. F., III (1992a) *Anal. Biochem. 203*, 295−301.
Stafford, W. F., III (1992b) *Analytical Ultracentrifugation in Biochemistry and Polymer Science* (Harding, S. E., Rowe, A. J., & Horton, J. C., Eds.) pp 359−353, Royal Society of Chemistry, Cambridge, UK.
Toso, R. J., Jordan, M. A., Farrell, K. W., Matsumoto, B., & Wilson, L. (1993) *Biochemistry 32*, 1285−1293.
Towbin, H., Staehlin, T., & Gordon, J. (1979) *Proc. Natl. Acad. Sci. U.S.A. 76*, 4350−4354.
Vandecandelaere, A., Martin, S. R., Schilstra, M. J., & Bayley, P. M. (1994) *Biochemistry 33*, 2792−2801.
Weber, G. (1975) *Adv. Protein Chem. 29*, 1−83.
Williams, R. C., Jr., & Lee, J. C. (1982) *Methods in Enzymology* (Frederiksen, D. W., & Cunningham, L. W., Eds.) Vol. 85, pp 376−408, Academic Press, New York.
Wilson, L., Jordan, M. A., Morse, A., & Margolis, R. L. (1982) *J. Mol. Biol. 159*, 125−149.

BI9502809